NANO LETTERS

Letter

pubs.acs.org/NanoLett

Design and Synthesis of Diverse Functional Kinked Nanowire Structures for Nanoelectronic Bioprobes

Lin Xu,[†,‡,§] Zhe Jiang,[‡,§] Quan Qing,[‡,§] Liqiang Mai,[†] Qingjie Zhang,[†] and Charles M. Lieber*[,†,‡,∥]

[†]WUT-Harvard Joint Nano Key Laboratory, State Key Laboratory of Advanced Technology for Materials Synthesis and Processing, Wuhan University of Technology, Wuhan 430070, China

[‡]Department of Chemistry and Chemical Biology and [∥]School of Engineering and Applied Sciences, Harvard University, Cambridge, Massachusetts 02138, United States

Supporting Information

ABSTRACT: Functional kinked nanowires (KNWs) represent a new class of nanowire building blocks, in which functional devices, for example, nanoscale field-effect transistors (nanoFETs), are encoded in geometrically controlled nanowire superstructures during synthesis. The bottom-up control of both structure and function of KNWs enables construction of spatially isolated point-like nanoelectronic probes that are especially useful for monitoring biological systems where finely tuned feature size and structure are highly desired. Here we present three new types of functional KNWs including (1) the zero-degree KNW structures with two parallel heavily doped arms of U-shaped structures with a nanoFET at the tip of the "U", (2) series multiplexed functional KNW integrating multi-nanoFETs along the arm and at the tips of V-shaped structures, and (3) parallel multiplexed KNWs integrating nanoFETs at the two tips of W-shaped structures. First, U-shaped KNWs were synthesized with separations as small as 650 nm between the parallel arms and used to fabricate three-dimensional nanoFET probes at least 3 times smaller than previous V-shaped designs. In addition, multiple nanoFETs were encoded during synthesis in one of the arms/tip of V-shaped and distinct arms/tips of W-shaped KNWs. These new multiplexed KNW structures were structurally verified by optical and electron microscopy of dopant-selective etched samples and electrically characterized using scanning gate microscopy and transport measurements. The facile design and bottom-up synthesis of these diverse functional KNWs provides a growing toolbox of building blocks for fabricating highly compact and multiplexed three-dimensional nanoprobes for applications in life sciences, including intracellular and deep tissue/cell recordings.

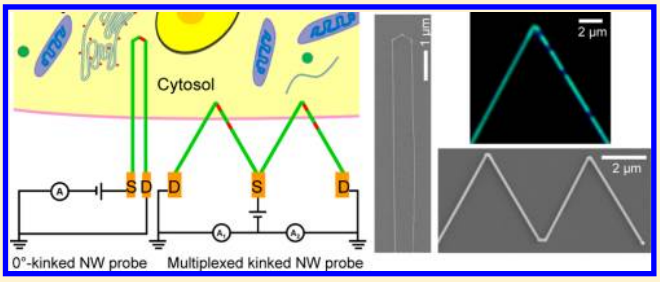

KEYWORDS: *Silicon nanowire, nanoprobe, nanosensor, field-effect transistor*

The rational design and synthesis of semiconductor nanowire (NW) building blocks with controlled structures have enabled the bottom-up fabrication paradigm with unprecedented flexibility to construct nanoelectronic and nanophotonic devices.[1−8] The development of NW structures from basic one-dimensional (1D)[9−11] through two- and three-dimensional (2D and 3D)[2,12−14] enables novel spatial and functional configurations of devices that have proven especially advantageous in developing nanoelectronic interfaces with biological systems.[13−21] In particular, functional KNWs in which nanoFETs or field sensitive p-n diodes are synthetically integrated in kinked NW superstructures have been used to fabricate 3D bend-up nanoelectronic probes to record extra- and intracellular action potentials from single cells and tissues.[14,20] In these nanobiosensors, the development of topological and compositional control in silicon NWs has enabled the synthesis and fabrication of single-detector probes from single 60° or 120° KNWs where the nanoscale detector is "presented" away from supporting substrates and bulky metal interconnects. However, the synthetic demonstration of more (i) complex NW geometries, including multikinked and zigzag-shaped NWs[14,20,22−31] and (ii) multiple nanoFETs within single 1D NWs[19,32] promise a rich combination of device designs that could open up distinct sensing applications. To realize this opportunity requires that several fundamental questions be addressed, including: (1) Can the probe size be reduced while at the same time being ca. size-independent away from the tip so that deep insertions are even less invasive; and (2) can ab initio design and subsequent synthesis be used to realize functional multiplexed KNW device arrays with defined geometry and topology?

Here we address these questions and substantially expand the scope of functional KNWs building blocks through the ab initio design and synthesis of several new structures as illustrated schematically in Figure 1. First, we designed U-shaped KNWs as compact, high aspect ratio probes (Figure 1a), where three 120° *cis*-kinks can define the "U", dopant modulation between two of these kinks defines nanoFET detector, and heavily doped (parallel) arms before/after the three kinks function as

Received: December 2, 2012

dx.doi.org/10.1021/nl304435z | *Nano Lett.* XXXX, XXX, XXX−XXX

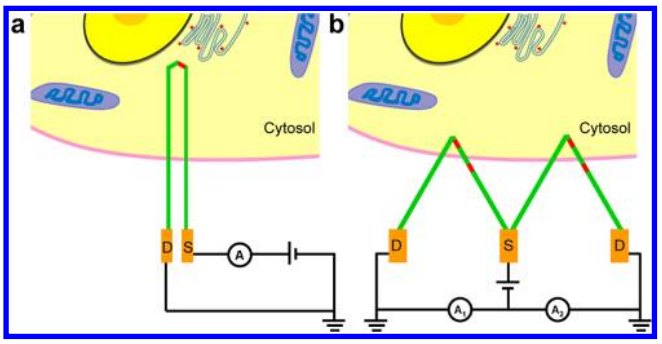

Figure 1. Overview of KNW synthetic designs and potential applications. (a) U-shaped KNW with integrated nanoFET (red) shown as a bioprobe for intracellular recording. (b) W-shaped KNW with multiple nanoFETs (red) illustrated as a bioprobe for simultaneous intracellular/extracellular recording. In a and b green indicates heavily doped (n^{++}) S/D NW nanoelectrode arms, red highlights the pointlike active nanoFET elements, and gold indicates the fabricated metal interconnects to the NW S/D arms. A schematic of a cell to scale is drawn with the different device designs to show the potential for achieving minimally invasive deep penetration (a) and multiplexed intracellular and extracellular recording (b).

nanoscale source/drain (S/D) connections to the FET. The width of this U-shaped KNW design is constant, determined by interkink segment lengths, and independent of the length of the arms. This design allows in principle deep penetration of the nanoFET detector into cells and tissue without increasing the cross-sectional area. Second, we have expanded upon our original V-shaped KNW with single detector by devising two approaches for encoding multiplexed nanoFET detectors (Figure 1b), where (i) dopant modulation is used to encode multiple FETs with controlled position and size along a single arm of a V-shaped KNW with the "V" defined by 1 or 2-*cis* 120° kinks, and (ii) dopant modulation is used to encode multiple FETs in distinct arms of W-shaped KNWs. These designs would allow for series and/or parallel multiplexing of intracellular/extracellular recording from a single nanobioprobe.

The KNWs were prepared using gold-nanoparticle (Au-NP) catalyzed vapor−liquid−solid (VLS) growth method with doping and geometric control adapted from our previous reports.[20,33] For the U-shaped KNWs (Figure 2a),[33] the initial heavily doped n^{++} straight arm was grown at 460 °C using 80 nm Au-NPs as the catalyst. Following typical 16 min arm growth (growth rate ca. 750 nm/min), the U-shape probe end was begun by introducing two 120° *cis*-kinks sequentially with the intervening NW segment grown for 100 s. After the second kink was initiated (by evacuation of the growth chamber), the nanoFET was encoded by reducing the phosphine dopant by 97.5% (from that used to prepare the heavily doped arms and initial turn of the "U") and growing a second segment for 100 s. Last, a third 120° *cis*-kink to complete the U-shaped end of the probe was introduced, and the other S/D arm was grown with the phosphine concentration at the initial high doping level.

A scanning electron microscopy (SEM) image of a typical Si KNW synthesized using the above procedure (Figure 2b, I) shows several key features. First, the overall U-shaped structure is obtained as a result of the *cis*-orientation of the three 120° kinks, including uniform parallel arms separated by ca. 2.1 μm. Second, the lengths of the two segments separating the kinks, 1.3 μm, which determines the observed arm separation, and the overall arm lengths, 12 μm, are consistent with programmed

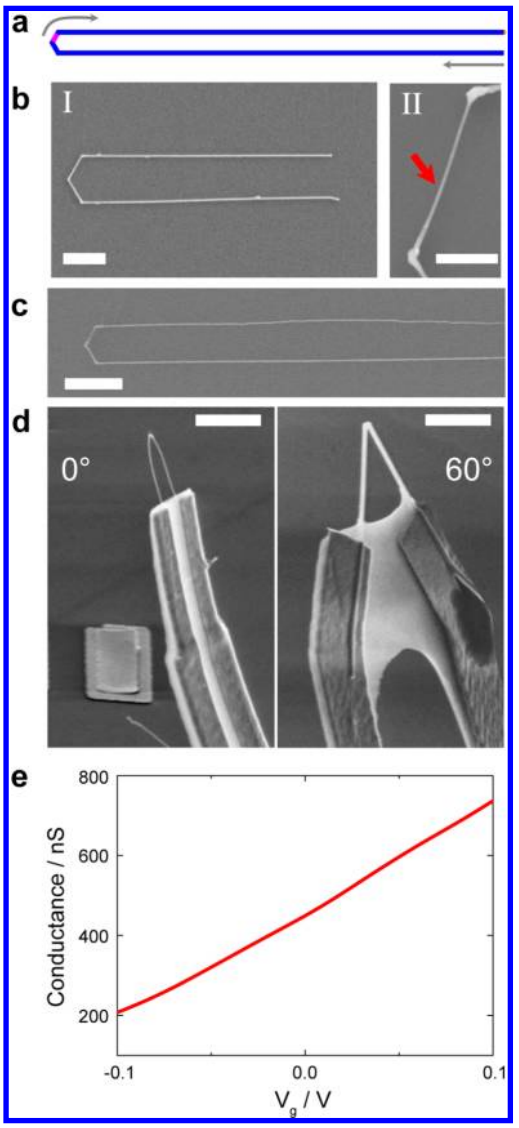

Figure 2. U-shaped KNWs. (a) Schematic of a U-shaped KNW with tip constructed from three 120° *cis*-linked kinks. The lightly doped n-type nanoFET element (pink) is encoded at the tip and connected by heavily doped n^{++} S/D arms (blue). The gray arrows indicate the growth sequence for the nanostructure. (b) SEM images of original (I: scale bare, 2 μm) and KOH-etched (II: scale bar, 500 nm) U-shaped KNW synthesized with 80 nm diameter Au-NP catalysts. The red arrow marks the position of nanoFET element between the second and the third cis-linked kinks. (c) Representative SEM image of a U-shaped KNW prepared using 30 nm diameter Au-NPs. The measured nanowire diameter is 30 nm. Scale bar, 1 μm. (d) SEM images of 3D probe devices fabricated using a 30 nm diameter U-shaped (left) and 150 nm diameter V-shaped (right) KNW building blocks. Scale bars, 3 μm. (e) Conductance versus water-gate reference potential data recorded from a representative 30 nm diameter U-shaped KNW 3D probe in 1× phosphate buffer saline (PBS).[37]

growth times during synthesis, thus showing that we could implement design changes in systematic manner (e.g., changing arm separation). To verify the designed dopant variation, which encodes the nanoFET detector, the U-shaped Si KNWs were etched with KOH solution,[34] where the KOH yields enhanced Si NW etching rates in regions with lower n-type dopant concentration.[11,19] An SEM image of the U-end of the same KNW after etching (Figure 2b, II) shows clearly the smaller NW diameter between the second and the third kinks and is

dx.doi.org/10.1021/nl304435z | *Nano Lett.* XXXX, XXX, XXX−XXX

thus consistent with the design and synthesis. The generality of this new KNW structure was further explored with the synthesis using a 2.7× smaller diameter Au-NP catalyst. A representative SEM image (Figure 2c) highlights this structure, where the separation between parallel 30 nm diameter arms of the "U" was reduced to only 650 nm. Overall, the yield of U-shaped KNW structures grown with both 80 and 30 nm catalysts was ca. 20%. Other "impurity" structures observed were straight or V-shaped NWs, thus suggesting that the kink yield (not *cis/trans* yield) is the factor that should be addressed to improve overall yields in the future.

We have used U-shaped KNWs to fabricate 3D devices to compare this new building block to previous V-shaped KNW nanoprobes and to characterize the electrical properties in solution. 3D devices were fabricated using stressed metal interconnects that bend the KNW probes upward after relief from the substrate.[20,35,36] Representative SEM images of U-shaped and V-shaped 3D KNW probes (Figure 2c) highlight the advantage of the U-shaped KNW for reducing overall probe cross-section as a function of distance from the probe end. Specifically, the U-shaped probe is no more than ∼1 μm in width at the point of the metal interconnects (3 μm total tip-to-contact length) compared to ∼4 μm width at similar point for the 60° V-shaped probe, and moreover, the total widths of the metal connections at the two KNW probes were <3 μm (U-shape) and ∼10 μm (V-shape). In addition, the U-shaped KNW probes could be further reduced in width through synthesis as discussed above and using higher resolution electron-beam lithography (EBL), while size reductions for the V-shaped probes are limited by structural geometry. In this regard, the U-shaped 3D KNW probes provide a better option for applications where deep insertion is desired. Second, the sensitivities of the nanoFET detectors encoded in the 3D U-shaped KNW probes were assessed in aqueous solution.[20,37] Representative conductance versus water-gate (Ag/AgCl electrode) data[37] (Figure 2e) yields a relatively linear n-type FET response with a sensitivity of 2.7 μS/V. Measurements on several U-shaped probes yields sensitivity values from ca. 1−10 μS/V and noise from ca. 1−4 mV (0−6000 Hz bandwidth), thus showing the capability to record both intracellular and extracellular signals from electrogenic cells.

In addition, we have used the V-shape KNW motif as a starting point to explore the integration of multiple nanoFETs to enable a multiplexed 3D bioprobes. The multiple nanoFETs were encoded in series along one arm of V-shaped KNWs (inset, Figure 3a) by dopant modulation,[33] where the overall yield of V-shaped KNWs was ca. 40%. A dark-field optical image of KOH-etched V-shaped KNW with four nanoFETs grown for 45 s/each and heavily doped segment growth times (between every two adjacent nanoFETs) following the initial nanoFET of 85, 170, and 340 s is shown in Figure 3a, where the KOH preferentially etches the lightly doped nanoFET regions.[11,19] The dark-field image shows clearly the four encoded nanoFETs (dark contrast) with ca. the same length and, moreover, shows that separation between nanoFETs along the arms increases as expected from the segment growth times. The nanoFET channel lengths and separations were quantified using SEM images (Figure 3b and Supporting Information, Figure S1), which yield FET lengths of 540, 550, 530, and 530 nm (from the KNW tip) and separations of 1.05, 2.03, and 4.08 μm. These results are consistent with the calibrated growth rate of ∼700 nm/min and demonstrate the capability for sophisticated bottom-up encoding of multiplexing function within the KNW building blocks.

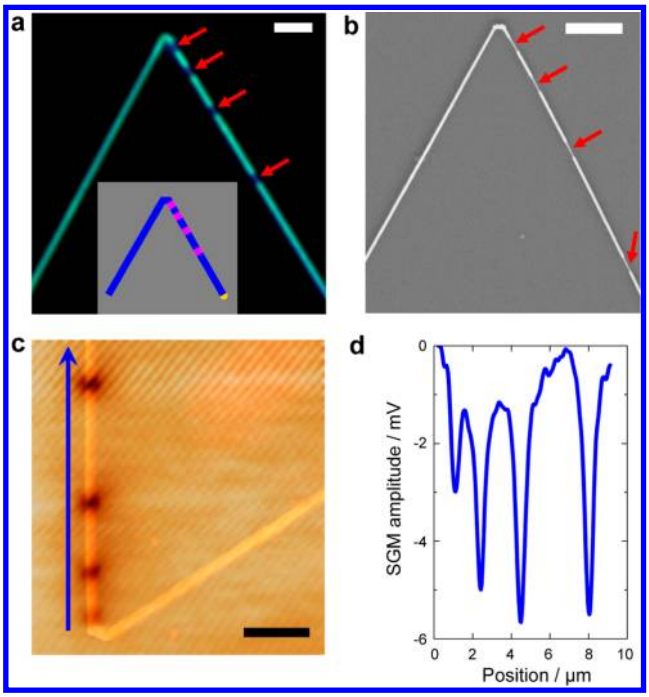

Figure 3. Series nanoFET in V-shaped KNWs. (a) Dark-field optical microscopy image of a KOH-etched KNW with 4 nanoFETs. The dark segments correspond to the four lightly doped nanoFET elements (red arrows). Scale bar, 2 μm. Inset, schematic of the synthetic design for the KNW with four series nanoFETs (pink) and heavily doped connecting NW segments (blue). (b) SEM image of the same KOH-etched KNW. Red arrows mark the positions of the preferentially etched lightly doped nanoFET channels. Scale bar, 2 μm. (c) Superposition of SGM and AFM topographic images for an unetched series KNW device, where the V-shaped KNW was synthesized in the same way as that shown in a and b; the tip voltage, V_{tip}, for the SGM image was −10 V. Scale bar, 2 μm. Dark regions in SGM image correspond to reduced NW conductance. (d) Line profile of the SGM signal along the NW arm indicated by the blue arrow in c. The negative peaks correspond to the dark regions in the SGM image.

The electrical characteristics of the series nanoFETs encoded in the arms of V-shaped KNWs were characterized using scanning gate microscopy (SGM).[32,38] Representative SGM and atomic force microscopy (AFM) images of a KNW device with four nanoFETs in series (Figure 3c and Supporting Information, Figure S2) highlight several key features. First, only the synthetically defined lightly doped regions showed gate response, indicating that the four series nanoFETs in this individual KNW can work independently as localized nanosensors. Second, the lengths of the lightly doped regions estimated from the full widths at half-maximum (fwhm) of the conductance line profile along the NW axis (Figure 3d) obtained from SGM were 502, 505, 510, and 505 nm, respectively. We note that these channel lengths calculated from SGM data agreed well with the results measured from KOH etched SEM images. Third, the positions of the SGM signal peaks matched the location of the four lightly doped FET elements revealed by KOH wet etch. Fourth, the amplitude variations determined from the SGM peaks suggest that sensitivities of the four distinct nanoFETs are within a factor of 2−3 of each other with the largest variation arising for the nanoFET closest to the tip of the KNW device. While further

dx.doi.org/10.1021/nl304435z | *Nano Lett.* XXXX, XXX, XXX−XXX

synthetic optimization should allow for series devices with comparable sensitivities to be prepared, taken together, the results demonstrate excellent bottom-up control of doping profile, active channel lengths, and positions of nanoFET elements in the KNW structures.

Last, we have extended the topological complexity of the original V-shaped KNW by designing and synthesizing W-shaped KNWs where one nanoFET detector is encoded at the tips of each of the two "Vs" making up the W-shaped structure (inset, Figure 4a). In this manner, independent, parallel

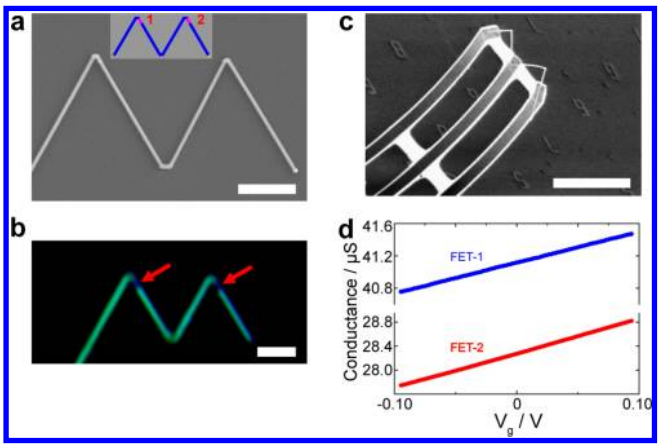

Figure 4. Parallel nanoFET KNWs. (a) SEM image of a W-shaped parallel-nanoFET KNW. Scale bar, 2 μm. Inset: Schematic of the W-shaped KNW with one nanoFET encoded at the tip of each V-shaped component of the "W", where blue and pink indicate heavily doped connections and lightly doped nanoFET channels, respectively. (b) Dark-field optical microscopy image of KOH etched W-shaped KNW. The two dark color segments correspond to the lightly doped nanoFET elements (red arrows) near the two tips. Scale bar, 2 μm. (c) SEM image of W-shaped parallel-nanoFET KNW bend-up probe. Scale bar, 20 μm. (d) Conductance versus water-gate reference potential data recorded independently from two parallel nanoFETs.

multiplexing with a single probe can be implemented (see below). The key structural feature needed to realize the W-shaped building block is *trans*-oriented kink at the central bend of the "W" relative to the two *cis*-kinks that define each of the V-shaped tip components of the structure. An SEM image of a W-shaped nanostructure (Figure 4a) highlights several key points. First, all of the bends defining the W-shape are defined by 60° angles at defined positions during growth. Second, each of the three 60° angles was introduced with two 120° *cis*-kinks with controlled tip widths of ca. 200 nm. Third, the 120° kinks separated by the ca. 4.5 μm arms have a *trans*-orientation as required to realize the "W" structure; we note that this is consistent with previous studies[20] that showed a higher yield of *trans* linkages was realized as the separation between 120° kinks was increased. Last, the overall yield of the W-shaped structure was ca. 10%, where other "impurity" structures typically had few numbers of kinks. This result suggests that as with the U-shaped probes overall yield could be improved in the future by increasing the yield of kink formation.

The positions of the nanoFETs encoded in the W-shaped were verified using the selective KOH etching described above. A representative dark-field optical microscopy image (Figure 4b) shows clearly that there is one lightly doped nanoFET at each probe tip and that the distance between the two nanoFET elements is ca. 4.5 μm. The spatial resolution of or separation between these parallel-nanoFETs, is determined by the length of the arms and the angle of the kinks. Currently the highest resolution is ~3 μm, although this could be further reduced to the submicrometer range by incorporating the zero-degree KNWs element at the central bend of the "W" or increased to ca. 10 μm by using a single 120° kink at this central bend.

To evaluate the multiplexing capability of the W-shaped KNW structures, we fabricated 3D probe devices where a common source connection was made to the central bend of the "W" and two independent drain connections were made to the outer arms of the structure.[35] A representative SEM image of W-shaped KNW probe connected in this manner (Figure 4c) shows that the probe bends upward uniformly from the substrate and presents both nanoFETs encoded in the two tips of the inverted "W" at the same height from the substrate. Water-gate measurements (Figure 4d) showed that the sensitivities of the two nanoFETs were 3.8 and 5.7 μS/V, which are comparable to the performance of single-kinked NW probes.[20] These results demonstrate that bottom-up designed parallel-nanoFETs in a single W-shaped KNW can work as independent multiplexed 3D nanosensors. We note that the key features of this unique multiplexed probe were all controlled during NW synthesis, which provides a potentially higher level of flexibility and precision compared to the postgrowth assembly of single-detector KNW devices.

In conclusion, we have designed and synthesized in good yield three new types of functional KNWs including (1) U-shaped KNW structures with two parallel heavily doped arms connecting a nanoFET at the tip of the "U", (2) series multiplexed functional KNW integrating multi-nanoFETs along the arm and at the tips of V-shaped structures, and (3) W-shaped multiplexed KNWs integrating nanoFETs at the two tips of W-shaped structures. The U-shaped KNWs were synthesized with parallel arm separations as small as 650 nm and were used to fabricate 3D nanoFET probes at least three times smaller than previous V-shaped designs. Second, four nanoFETs were encoded in precise positions by synthesis in one arm/tip of V-shaped building blocks, and SGM measurements demonstrated that the series detectors had similar sensitivities that have potential for recording both extracellular and intracellular action potentials. Third, two nanoFETs were encoded in distinct arms of the new W-shaped KNW, and these building blocks were used to fabricate 3D nanoprobes capable of parallel multiplexing measurements using the independently addressable nanoFET detectors. The facile design and bottom-up synthesis of these diverse functional KNWs provides a greatly expanded toolbox of building blocks for fabricating highly compact and multiplexed three-dimensional nanoprobes for applications in life sciences, including (1) deep intracellular and deep tissue recordings with the ultrasmall U-shaped probes, (2) series multiplexed recording, for example for simultaneous intracellular and extracellular responses, using the new V-shaped probes having detectors spatially encoded along a single arm, and (3) parallel multiplexing, for example for simultaneous, independent recording of at least two intracellular signals from spatially defined positions within a single cell.

■ ASSOCIATED CONTENT

Supporting Information

Additional information and figures. This material is available free of charge via the Internet at http://pubs.acs.org.

dx.doi.org/10.1021/nl304435z | *Nano Lett.* XXXX, XXX, XXX–XXX

AUTHOR INFORMATION

Corresponding Author

*E-mail: cml@cmliris.harvard.edu.

Author Contributions

[§]These authors contributed equally to this work.

Notes

The authors declare no competing financial interest.

ACKNOWLEDGMENTS

Work at Wuhan University of Technology was supported by the National Basic Research Program of China (2013CB934103, 2012CB933003), the National Natural Science Foundation of China (51272197, 51072153), Program for New Century Excellent Talents in University (NCET-10-0661), the International S&T Cooperation (2013ZR02930), and the Fundamental Research Funds for the Central Universities (2011-YB-01). Research at Harvard was supported by NIH Director's Pioneer (1DP1OD003900) and DOD NSSEFF (N00244-09-1-0078) Awards.

REFERENCES

(1) Lieber, C. M. *MRS Bull.* **2011**, *36*, 1052−1063.
(2) Tian, B.; Lieber, C. M. *Pure Appl. Chem.* **2011**, *83*, 2153−2169.
(3) Schmidt, V.; Wittemann, J. V.; Gosele, U. *Chem. Rev.* **2010**, *110*, 361−388.
(4) Mai, L.; Yang, F.; Zhao, Y.; Xu, X.; Xu, L.; Hu, B.; Luo, Y.; Liu, H. *Mater. Today* **2011**, *14*, 346−353.
(5) Wang, Z. L. *MRS Bull.* **2012**, *37*, 814−827.
(6) Wu, H.; Cui, Y. *Nano Today* **2012**, *7*, 414−429.
(7) Yang, P. *MRS Bull.* **2012**, *37*, 806−813.
(8) Wacaser, B. A.; Dick, K. A.; Johansson, J.; Borgstrom, M. T.; Deppert, K.; Samuelson, L. *Adv. Mater.* **2009**, *21*, 153−165.
(9) Yan, H.; Choe, H. S.; Nam, S. W.; Hu, Y.; Das, S.; Klemic, J. F.; Ellenbogen, J. C.; Lieber, C. M. *Nature* **2011**, *470*, 240−244.
(10) Tian, B.; Zheng, X.; Kempa, T. J.; Fang, Y.; Yu, N.; Yu, G.; Huang, J.; Lieber, C. M. *Nature* **2007**, *449*, 885−890.
(11) Kempa, T. J.; Tian, B.; Kim, D. R.; Hu, J.; Zheng, X.; Lieber, C. M. *Nano Lett.* **2008**, *8*, 3456−3460.
(12) Jiang, X.; Tian, B.; Xiang, J.; Qian, F.; Zheng, G.; Wang, H.; Mai, L.; Lieber, C. M. *Proc. Natl. Acad. Sci. U.S.A.* **2011**, *108*, 12212−12216.
(13) Duan, X.; Gao, R.; Xie, P.; Cohen-Karni, T.; Qing, Q.; Choe, H. S.; Tian, B.; Jiang, X.; Lieber, C. M. *Nat. Nanotechnol.* **2012**, *7*, 174−179.
(14) Jiang, Z.; Qing, Q.; Xie, P.; Gao, R.; Lieber, C. M. *Nano Lett.* **2012**, *12*, 1711−1716.
(15) Zheng, G.; Patolsky, F.; Cui, Y.; Wang, W. U.; Lieber, C. M. *Nat. Biotechnol.* **2005**, *23*, 1294−1301.
(16) Xie, C.; Lin, Z.; Hanson, L.; Cui, Y.; Cui, B. *Nat. Nanotechnol.* **2012**, *7*, 185−190.
(17) Yan, R.; Park, J. H.; Choi, Y.; Heo, C. J.; Yang, S. M.; Lee, L. P.; Yang, P. *Nat. Nanotechnol.* **2012**, *7*, 191−196.
(18) Gao, R.; Strehle, S.; Tian, B.; Cohen-Karni, T.; Xie, P.; Duan, X.; Qing, Q.; Lieber, C. M. *Nano Lett.* **2012**, *12*, 3329−3333.
(19) Cohen-Karni, T.; Casanova, D.; Cahoon, J. F.; Qing, Q.; Bell, D. C.; Lieber, C. M. *Nano Lett.* **2012**, *12*, 2639−2644.
(20) Tian, B.; Cohen-Karni, T.; Qing, Q.; Duan, X.; Xie, P.; Lieber, C. M. *Science* **2010**, *329*, 830−834.
(21) Qing, Q.; Pal, S. K.; Tian, B.; Duan, X.; Timko, B. P.; Cohen-Karni, T.; Murthy, V. N.; Lieber, C. M. *Proc. Natl. Acad. Sci. U.S.A.* **2010**, *107*, 1882−1887.
(22) Tian, B.; Xie, P.; Kempa, T. J.; Bell, D. C.; Lieber, C. M. *Nat. Nanotechnol.* **2009**, *4*, 824−829.
(23) Musin, I. R.; Filler, M. A. *Nano Lett.* **2012**, *12*, 3363−3368.
(24) Lee, G.; Woo, Y. S.; Yang, J. E.; Lee, D.; Kim, C. J.; Jo, M. H. *Angew. Chem., Int. Ed.* **2009**, *48*, 7366−7370.
(25) Lugstein, A.; Steinmair, M.; Hyun, Y. J.; Hauer, G.; Pongratz, P.; Bertagnolli, E. *Nano Lett.* **2008**, *8*, 2310−2314.
(26) Madras, P.; Dailey, E.; Drucker, J. *Nano Lett.* **2009**, *9*, 3826−3830.
(27) Ben-Ishai, M.; PatoLsky, F. *Nano Lett.* **2012**, *12*, 1121−1128.
(28) Geaney, H.; Dickinson, C.; Weng, W.; Kiely, C. J.; Barrett, C. A.; Gunning, R. D.; Ryan, K. M. *Cryst. Growth Des.* **2011**, *11*, 3266−3272.
(29) Schwarz, K. W.; Tersoff, J. *Nano Lett.* **2011**, *11*, 316−320.
(30) Ross, F. M. *Rep. Prog. Phys.* **2010**, *73*, 114501 (21pp).
(31) Kim, J. H.; Moon, S. R.; Kim, Y.; Chen, Z. G.; Zou, J.; Choi, D. Y.; Joyce, H. J.; Gao, Q.; Tan, H. H.; Jagadish, C. *Nanotechnology* **2012**, *23*, 115603 (6pp).
(32) Yang, C.; Zhong, Z.; Lieber, C. M. *Science* **2005**, *310*, 1304−1307.
(33) The three types of functional KNWs described in this paper were synthesized as follows. (1) The U-shaped KNWs were synthesized by chemical vapor deposition (CVD) through a nanoparticle-catalyzed VLS process as described previously.[20] Specifically, 30, 80, or 150 nm diameter Au-NPs (Ted Pella) were dispersed on Si growth substrates with 600 nm SiO_2 layer (Nova Electronic Materials). Growth of heavily phosphorous-doped n-type arm was first carried out by feeding SiH_4 (1 sccm, 99.9999%), PH_3 (4 sccm, 1000 ppm in H_2), and H_2 (60 sccm) into the system (atom ratio of Si:P is 250:1) for 16 min at a total pressure of 40 Torr and temperature of 460 °C. The growth was then paused for 15 s to introduce one 120° kink, by rapidly evacuating the chamber to lowest pressure and shutting off the gas lines. The following two 120° *cis*-kinks were introduced via the same procedure, with a 40−100 s growth time between every two *cis*-linked kinks. To grow the lightly doped n-type FET segment between the second and the third 120° *cis*-kinks at the tip, the flow rates of SiH_4 (99.9999%) and PH_3 (1000 ppm in H_2) were 1 and 0.5 sccm (atom ratio of Si:P is 2000:1, for 30 nm diameter nanowires) or 1 and 0.1 sccm (atom ratio of Si:P is 10,000:1 for 80 and 150 nm diameter nanowires). Finally, the second heavily doped n-type arm was allowed to finish in additional 16 min. (2) Series multi-nanoFET KNWs were grown with reactant gas flow rates, total gas pressure, and growth temperature the same to U-shaped KNWs described in (1). Initially, the first heavily doped n^{++} arm (atom ratio of Si:P is 250:1) was grown for 30 min, and the reactor was then evacuated for 15 s to introduce a 120° kink, then the n^{++} tip segment was grown for 20 s followed by evacuating the reactor for 15 s again to introduce another 120° cis-linked kink. The lightly doped nanoFET segments (atom ratio of Si:P is 10,000:1) with intentionally varied distance were grown and encoded in the second n^{++} arm, in which the growth time for each nanoFET element was 45 s, and growth times for the n^{++} segment between two adjacent nanoFETs were 85, 170, and 340 s, respectively. The total growth time of the second arm was 30 min. Dopant modulation was achieved by varying the flow rates of PH_3 (1000 ppm in H_2) at 4 and 0.1 sccm for heavily doped n^{++}- and lightly doped n-type segments respectively and kept the flow rates of SiH_4 (1 sccm, 99.9999%) and H_2 (60 sccm) constant. (3) The growth temperature and reactant gas pressures of parallel-nanoFET multi-kinked NWs were the same to U-shaped KNWs described in (1). Specifically, using 150 nm diameter gold catalysts, the four heavily doped n^{++} arms (atom ratio of Si:P is 250:1) were grown for 6−18 min, respectively (Initial arm was grown 10 min longer than other three arms), and all adjacent arms were connected by a 60° tip constructed from two *cis*-linked 120° kinks. Lightly doped nanoFET elements (atom ratio of Si:P is 10,000:1) with growth time of 45 s were introduced immediately after each probe tip growth. Dopant modulation was achieved by varying the flow rates of PH_3 (1000 ppm in H_2) at 4 and 0.1 sccm for heavily doped n^{++}- and lightly doped n-type segments, respectively, and the flow rates of SiH_4 (1 sccm, 99.9999%) and H_2 (60 sccm) were kept constant.
(34) We used KOH selective wet etching to analyze the doping profile of the KNWs encoded with nanoFETs. Briefly, 10 g of KOH (Sigma-Aldrich Inc.) was dissolved in 88 mL of deionized H_2O and 37 mL of isopropanol. Substrates with dispersed NWs were dipped in buffered hydrogen fluoride (BHF) solution (Transene Company Inc.)

for 10 s followed with deionized H_2O rinse and then immediately dipped in this KOH solution for 3−10 s at 50−60 °C. The substrates were rinsed with deionized H_2O, followed with isopropanol rinse and N_2 blow drying.

(35) The bend-up probes were fabricated on Si substrates (Nova Electronic Materials, n-type 0.005 Ω cm) with 600 nm SiO_2 layer. A nickel sacrificial layer (100 nm) was first defined by EBL and thermal evaporation. The substrate was then coated with SU-8 resist (2000.5, MicroChem Corp.), on which the as-synthesized KNWs suspended in ethanol were deposited. After definition of the bottom SU-8 support layer by EBL, S/D metal contacts were defined by EBL and metalized by thermal evaporation of Ti/Pd/Ti (1.5/120/60 nm). Typically, the S/D contact separation was 0.5−1 μm for U-shaped KNW probe and 10−15 μm for V-shaped KNW probe, and the free end of the NW extended 3−4 μm from the source contact. The top SU-8 layer was subsequently defined by EBL for passivation. Etching of the nickel sacrificial layer (∼1 h) in nickel etchant (TFB, Transene Company, Inc.) yielded the 3D bend-up probes.

(36) Tian, B.; Liu, J.; Dvir, T.; Jin, L.; Tsui, J. H.; Qing, Q.; Suo, Z.; Langer, R.; Kohane, D. S.; Lieber, C. M. *Nat. Mater.* **2012**, *11*, 986−994.

(37) The water-gate measurements were carried out in 1× phosphate buffer saline (PBS). An Ag/AgCl wire was used as a reference electrode. The KNW device conductance was measured with dc bias set to 0.1 V, and the current was converted to voltage with a current preamplifier (Model 1211, DL Instruments) at sensitivity of 10^{-6} A/V, before low-pass filtered (0−6 kHz, CyberAmp 380, Molecular Devices) and digitized at 20 kHz sampling rate (Axon Digi1440A, Molecular Devices).

(38) The device chip was mounted on a BioScope MultiMode SPM stage (Digital Instrument). The S/D voltage across the device was kept constant at 0.1 V, and S/D current was measured using a low-noise differential preamplifier (SR560, Stanford Research Systems). The device conductance was calculated from S/D voltage and current. A conductive AFM tip (PPP-NCHPt, Nanosensors) was used as a local gate and scanned over the device to map the conductance image in "Lift Mode". Specifically, first, for each scan line, zero potential was applied to the tip, and a topographic image was acquired in Tapping Mode with feedback enabled. The tip was then lifted up 30 nm, and a tip potential of ±10 V was applied. The tip was scanned across the same line again following the captured topological profile with feedback turned off, when the change of conductance of the device was recorded.